

---

**Pacific Northwest  
National Laboratory**

Operated by Battelle for the  
U.S. Department of Energy

**Spent Fuel Drying System Test Results  
(Dry-Run in Preparation for Run 8)**

B. M. Oliver  
G. S. Klinger  
J. Abrefah

S. C. Marschman  
P. J. MacFarlan  
G. A. Ritter

July 1999

RECEIVED

AUG 23 1999

STI



Prepared for the U.S. Department of Energy  
under Contract DE-AC06-76RLO 1830

---

## DISCLAIMER

This report was prepared as an account of work sponsored by an agency of the United States Government. Neither the United States Government nor any agency thereof, nor Battelle Memorial Institute, nor any of their employees, makes any warranty, express or implied, or assumes any legal liability or responsibility for the accuracy, completeness, or usefulness of any information, apparatus, product, or process disclosed, or represents that its use would not infringe privately owned rights. Reference herein to any specific commercial product, process, or service by trade name, trademark, manufacturer, or otherwise does not necessarily constitute or imply its endorsement, recommendation, or favoring by the United States Government or any agency thereof, or Battelle Memorial Institute. The views and opinions of authors expressed herein do not necessarily state or reflect those of the United States Government or any agency thereof.

PACIFIC NORTHWEST NATIONAL LABORATORY

*operated by*

BATTELLE

*for the*

UNITED STATES DEPARTMENT OF ENERGY

*under Contract DE-AC06-76RLO 1830*

Printed in the United States of America

Available to DOE and DOE contractors from the  
Office of Scientific and Technical Information, P.O. Box 62, Oak Ridge, TN 37831;  
prices available from (615) 576-8401.

Available to the public from the National Technical Information Service,  
U.S. Department of Commerce, 5285 Port Royal Rd., Springfield, VA 22161



This document was printed on recycled paper.

## **Spent Fuel Drying System Test Results (Dry-Run in Preparation for Run 8)**

B. M. Oliver	S. C. Marschman
G. S. Klinger	P. J. MacFarlan
J. Abrefah	G. A. Ritter

July 1999

Prepared for  
the U.S. Department of Energy  
under Contract DE-AC06-76RLO 1830

Pacific Northwest National Laboratory  
Richland, Washington 99352



## **DISCLAIMER**

**Portions of this document may be illegible in electronic image products. Images are produced from the best available original document.**

## Summary

N-Reactor fuel elements, which had been stored underwater in the Hanford 100 Area K-West Basin, have been subjected to a combination of low- and high-temperature vacuum drying treatments. These studies are part of a series of tests being conducted by Pacific Northwest National Laboratory on the drying behavior of spent nuclear fuel elements removed from both the K-West and K-East Basins.

The drying test series was designed to test fuel elements that ranged from intact to severely damaged. This report describes the results of a dry-run of the test procedure prior to the testing of the eighth and final fuel element in the series, Element 6513U. The reasons for performing this third dry-run included new calibrations of the argon flow controller and the gas chromatograph and changes in the system configuration.

The dry-run test was conducted in the Whole Element Furnace Testing System located in G-Cell within the Postirradiation Testing Laboratory (PTL). This test system is composed of three basic systems: the in-cell furnace equipment, the system gas loop, and the analytical instrument package. The dry-run test consisted of drying processes based on those proposed under the Integrated Process Strategy, and included a hot drying step. The test cycles are listed below:

- Cold Vacuum Drying (CVD) at  $\sim 50^{\circ}\text{C}$  under vacuum ( $\sim 19$  hr)
- Pressure Rise Test at  $\sim 50^{\circ}\text{C}$  ( $\sim 1$  hr)
- Hot Vacuum Drying (HVD) for a total of  $\sim 67$  hr ( $\sim 25$  hr at  $\sim 75^{\circ}\text{C}$ ,  $\sim 34$  hr at  $\sim 75^{\circ}\text{C}$  to  $\sim 400^{\circ}\text{C}$ , and  $\sim 8$  hr at  $\sim 400^{\circ}\text{C}$ )
- System Cooldown to  $\sim 50^{\circ}\text{C}$  ( $\sim 53$  hr)
- Post-Test Pressure Rise Test at  $\sim 50^{\circ}\text{C}$  ( $\sim 1$  hr).

Prior to CVD, 10 ml of water were added to the system using a graduated cylinder. Approximately 3 ml of water were observed in the condenser during the condenser pumpdown phase of CVD, somewhat higher than a value of  $\sim 1.4$  g calculated over the same time period. Review of previous drying test data suggested that the cause of the incomplete water recovery in the condenser was due to the shorter duration of the condenser pumpdown phase combined with hang-up of water in colder sections of the system. Run 7 (Element 2660M), which had a much longer condenser phase, showed significantly higher fractional water recovery.

The observed pressure rise during the post-CVD Pressure Rise Test was  $\sim 0.4$  Torr/hr, below the acceptance criterion of 0.5 Torr/hr. Similar to earlier tests, the total pressure rise observed in the post-CVD test was only partially caused by residual moisture, suggesting that other sources of gas are responsible for some of the total pressure rise. Approximately 1 mg of water was calculated to have been

removed during the Pressure Rise Test. This water can likely be interpreted as coming from free water that was trapped in isolated regions of the furnace system and not completely removed during CVD.

Water removal during the three phases of HVD was  $\sim 0.2$  g,  $\sim 0.05$  g, and  $\sim 0.004$  g, respectively. A small water release peak was observed during HVD-2 at  $\sim 170^\circ\text{C}$ . Water released during HVD is attributed largely to the release of water from isolated regions of the furnace system. Approximately 6 mg of water were released during post-HVD cooldown, indicating small residual quantities of water remaining even after the drying test was completed.

Hydrogen was observed during the test during the condenser pumpdown phase of CVD and during HVD. Hydrogen observed was only  $\sim 0.001$  mg during CVD, and  $\sim 0.2$  mg during HVD. These levels are about three orders of magnitude lower than observed during actual fuel element drying, and represent background hydrogen outgassing rates for the furnace system.

## Quality Assurance

This work was conducted under the Quality Assurance Program, Pacific Northwest National Laboratory (PNNL) SNF-70-001, *SNF Quality Assurance Program*, as implemented by the PNNL *SNF Characterization Project Operations Manual*. This QA program has been evaluated and determined to effectively implement the requirements of DOE/RW-0333P, Office of Civilian Radioactive Waste Management *Quality Assurance Requirements and Description (QARD)*. Compliance with the QARD is mandatory for projects that generate data used to support the development of a permanent High-Level Nuclear Waste repository. Further, the U.S. Department of Energy has determined that the testing activities which generated the results documented in this report shall comply with the QARD. Supporting records for the data in this report are located in the permanent PNNL SNF Characterization Project records, *Wet/Dry Run Testing of G-Cell Furnace System in Preparation for Run #8 (6513U)*.





# Contents

Summary .....	iii
Quality Assurance .....	v
Acronyms .....	xi
1.0 Introduction .....	1.1
2.0 Whole Element Furnace Testing System .....	2.1
2.1 Major Systems Overview .....	2.1
2.2 Vacuum Pumping System .....	2.4
2.2.1 Varian Scroll Pump .....	2.4
2.2.2 Water Condenser .....	2.5
2.2.3 Piping, Valves, and Filters.....	2.5
2.2.4 System Line Heaters.....	2.5
2.3 Process Heating System .....	2.7
2.4 Gas Supply/Distribution System .....	2.7
2.5 Gas Analysis Instrumentation .....	2.8
2.5.1 Balzers Omnistar Mass Spectrometer .....	2.8
2.5.2 MTI M200 Gas Chromatograph.....	2.9
2.6 Process Instrumentation .....	2.9
2.6.1 Vaisala Moisture Monitor.....	2.9
2.6.2 Panametrics Moisture Monitor .....	2.10
2.6.3 MKS Baratron Pressure Transducers .....	2.10
2.6.4 Cole-Parmer Pressure Transducer .....	2.11

2.6.5 Thermocouples .....	2.12
2.7 Data Acquisition and Control System .....	2.12
3.0 Vacuum Drying Testing of Furnace System .....	3.1
3.1 Initial Conditions .....	3.1
3.2 System Drying.....	3.1
3.2.1 Cold Vacuum Drying .....	3.3
3.2.2 Pressure Rise Test .....	3.4
3.2.3 Hot Vacuum Drying, Step 1 .....	3.4
3.2.4 Hot Vacuum Drying, Step 2 .....	3.4
3.2.5 Hot Vacuum Drying, Step 3 .....	3.4
3.2.6 System Cooldown and Post-Test Pressure Rise Test .....	3.4
3.3 Calculation of Water and Hydrogen Inventories.....	3.5
4.0 Experimental Results.....	4.1
4.1 Cold Vacuum Drying .....	4.1
4.2 Pressure Rise Tests.....	4.3
4.3 Hot Vacuum Drying .....	4.8
4.4 Gas Chromatograph Measurements .....	4.8
4.5 Mass Spectrometer Measurements.....	4.14
5.0 Discussion .....	5.1
6.0 References .....	6.1
7.0 Supporting Documents and Related Reports.....	7.1

## Figures

2.1 Fuel Element Drying System Components (in-cell).....	2.2
2.2 Fuel Element Drying System Components (ex-cell).....	2.3
2.3 Generalized View of Test System .....	2.6
4.1 Spent Fuel Drying System Test Results, Summary Plot .....	4.2
4.2 Spent Fuel Drying System Test Results, Cold Vacuum Drying.....	4.4
4.3 Spent Fuel Drying System Test Results, Post-CVD Pressure Rise Test .....	4.5
4.4 Spent Fuel Drying System Test Results, Post-HVD Pressure Rise Test.....	4.6
4.5 Spent Fuel Drying System Test Results, Hot Vacuum Drying – Step 1 .....	4.9
4.6 Spent Fuel Drying System Test Results, Hot Vacuum Drying – Step 2 .....	4.10
4.7 Spent Fuel Drying System Test Results, Hot Vacuum Drying – Step 3 .....	4.11
4.8 Spent Fuel Drying System Test Results, Hydrogen Release During CVD .....	4.12
4.9 Spent Fuel Drying System Test Results, Hydrogen Release During HVD and Cooldown .....	4.13

## Tables

2.1 Water and Ice Vapor Pressure Data Versus Temperature .....	2.11
3.1 Summary of Nominal Test Design Conditions .....	3.2
4.1 Dry-Run Time Line .....	4.3



## Acronyms

ATS	Applied Test Systems
CVD	Cold Vacuum Drying
DACS	data acquisition and control system
DP	dew point
ET	elapsed time
GC	gas chromatograph
HP	Hewlett Packard
HVD	Hot Vacuum Drying
ID	inside diameter
IPS	Integrated Process Strategy
MS	mass spectrometer
NIST	National Institute of Standards and Technology
OD	outside diameter
PNNL	Pacific Northwest National Laboratory
PTL	Postirradiation Testing Laboratory
QA	Quality Assurance
QARD	Quality Assurance Requirements and Description
SFEC	single fuel element canister
SNF	spent nuclear fuel
UHP	ultra high purity
VP	vapor pressure

## 1.0 Introduction

The water-filled K-Basins in the Hanford 100 Area have been used to store N-Reactor spent nuclear fuel (SNF) since the 1970s. Because some leaks in the basin have been detected and some of the fuel is breached due to handling damage and corrosion, efforts are underway to remove the fuel elements from wet storage. An Integrated Process Strategy (IPS) has been developed to package, dry, transport, and store these metallic uranium fuel elements in an interim storage facility on the Hanford Site (WHC 1995). Information required to support the development of the drying processes, and the required safety analyses, is being obtained from characterization tests conducted on fuel elements removed from the K-Basins. A series of whole element drying tests (reported in separate documents, see Section 7.0) have been conducted by Pacific Northwest National Laboratory (PNNL)<sup>(a)</sup> on several intact and damaged fuel elements recovered from both the K-East and K-West Basins.

This report documents the results of a test "dry-run" conducted prior to the eighth and last of those tests, which was conducted on an N-Reactor outer fuel element removed from K-West canister 6513U. The system used for the dry-run test was the Whole Element Furnace Testing System, described in Section 2.0, located in the Postirradiation Testing Laboratory (PTL, 327 Building). The test conditions and methodologies are given in Section 3.0. The experimental results are provided in Section 4.0 and discussed Section 5.0.

---

(a) Operated by Battelle for the U.S. Department of Energy under Contract DE-AC06-76RLO 1830.

## 2.0 Whole Element Furnace Testing System

A complete description for the Whole Element Furnace Testing System, including detailed equipment specifications, is provided in Ritter et al. (1998). Some changes were made to the system configuration prior to the present test run. These included new calibrations for the system gas chromatograph (GC) and mass spectrometer (MS), and the addition of several new pressure and moisture sensors. These modifications are discussed in the following systems overview.

### 2.1 Major Systems Overview

An overview of the furnace testing system is presented in this section. The subsystems pertinent to this test report are as follows:

- **Vacuum Pumping System** - This system consists of a scroll-type vacuum pump, a condenser with chiller, filters, valves, and piping, which provide the vacuum pressures and flows required for the proposed IPS vacuum processes.
- **Process Heating System** - This system consists of a resistively heated, clam-shell furnace and a sample chamber (retort) to provide heating to the fuel element and to control process temperatures.
- **Gas Supply/Distribution System** - This system consists of gas bottles; mass flow controllers; piping; and valves for metering argon, air, or oxygen through the system. A bubbler is also available for adding water vapor to the system if desired.
- **Gas Analysis Instrumentation** - The gas analysis instrumentation includes a 300-amu quadrupole MS and a GC for monitoring selected elements in the process gas stream.
- **Process Instrumentation** - The system is equipped with several instruments for measuring process temperatures, pressures, and moisture level. An auxiliary turbo vacuum pumping system provides low system pressures for zero adjustment of the high accuracy retort pressure sensor.
- **Data Acquisition and Control System (DACS)** - The DACS consists of an IBM-compatible computer and data acquisition/control unit to monitor/store key system parameters (temperatures, pressures, flows, moisture level), along with controlling the process heating system and a safety argon system.

Figures 2.1 and 2.2 are photographs of the equipment located inside and outside of G-Cell. The furnace (including retort) and some of the process piping, instrumentation, and valves are located inside the hot cell. The furnace sits on the cell floor, and the process piping is routed to a rack that hangs on the west cell wall. Process piping, electrical power, and instrumentation wires pass through several split plugs on the west side of the cell. The process piping on the outside of the cell is contained within a glove bag, which provides a secondary containment as a precaution in case the process piping lines





Figure 2.1. Fuel Element Drying System Components (in-cell)

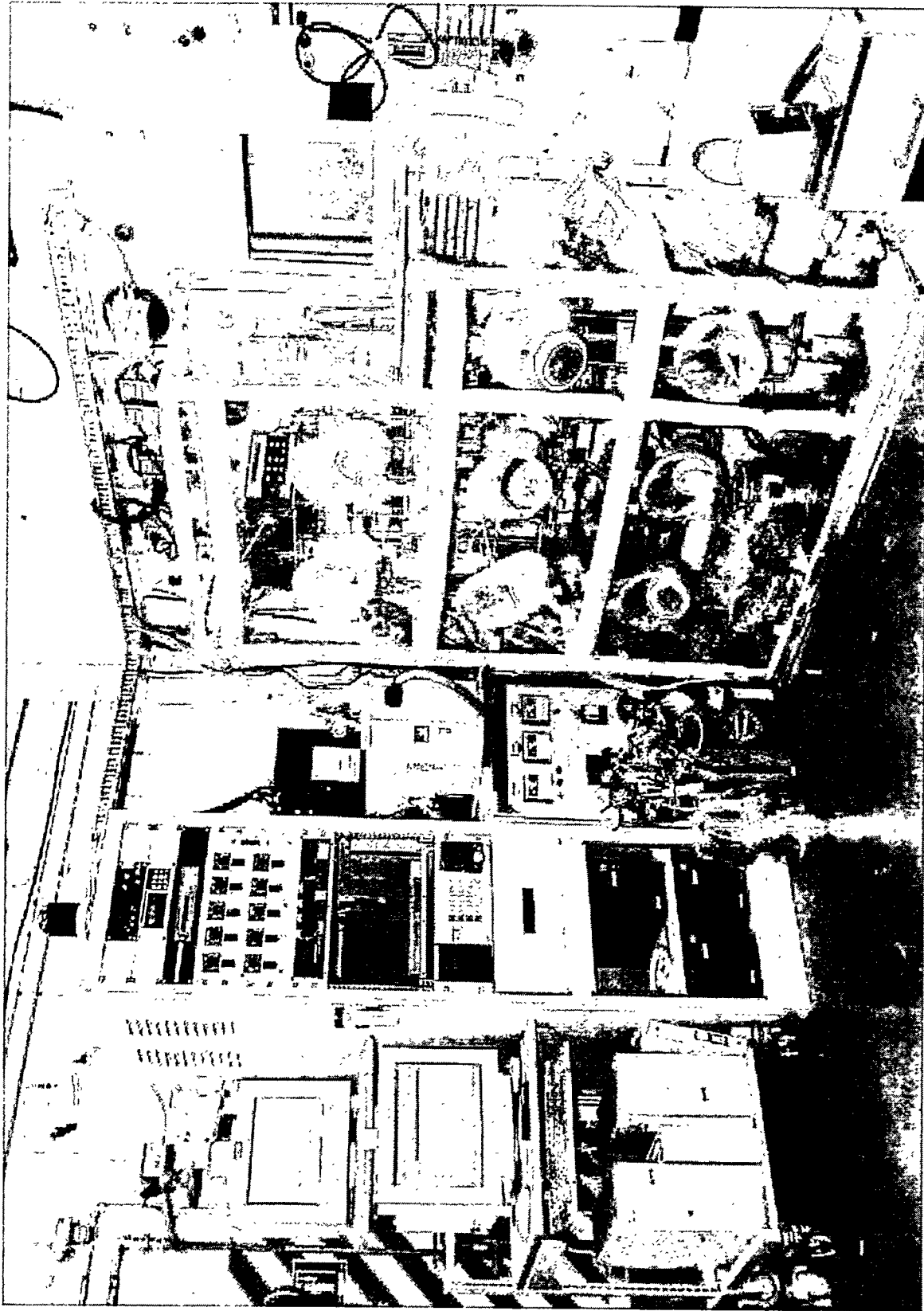


Figure 2.2. Fuel Element Drying System Components (ex-cell)

become contaminated. The vacuum pump, condenser, bubbler, GC, and the remainder of the instrumentation and valves are located inside this glove bag. Instrumentation and electrical power wires are routed through pass-through sleeves on the sides of the glove bag to the instrument rack and computer console.

The instrument rack contains the readout/control units for the pressure sensors, moisture sensor, and flow controllers, along with the heat trace temperature controllers, data acquisition/control unit, turbo pump controller, GC laptop computer, and uninterruptible power supplies. The computers for the DACS and MS are located next to the instrument rack. The following sections provide more detailed descriptions of the components for these subsystems.

## **2.2 Vacuum Pumping System**

The vacuum pumping system provides the pressures and flows required for the proposed IPS processes. This system connects the furnace retort with all the other components of the test system through various valves, fittings, and piping. The vacuum pumping system consists of the following components:

- scroll pump for evacuating the system to pressures below 1 Torr
- water condenser with refrigerated chiller for gross removal of water
- valves and piping for connecting the various components and controlling the flow direction
- particulate filters to prevent the spread of contamination
- heating cords with temperature controllers for preventing condensation in lines.

### **2.2.1 Varian Scroll Pump**

The system vacuum pump is a Varian model 300DS scroll pump. This pump has an ultimate vacuum pressure less than  $10^{-2}$  Torr and a peak pumping speed of 250 l/min (8.8 cfm). These pressures and flows are more than adequate for simulating the conditions of the proposed IPS vacuum processes. For a single fuel element, this amount of flow may be more than desired. Therefore, a metering valve was installed on the pump inlet to throttle the flow to lower levels as required. The desired system pressure is achieved by either using the metering valve or flowing ultra high purity (UHP) argon into the system through the entire gas loop or via a direct injection of ballast gas at the pump inlet. The use of argon gas helps to prevent the in-leakage of moisture-containing air through small system leaks (which are difficult to eliminate) that would interfere with process monitoring equipment.

### **2.2.2 Water Condenser**

The scroll vacuum pump can be damaged by condensation of liquid water in the scroll mechanism, and, since each element was wet at the start of each test, the possibility of pump damage was considered. A water condenser with corresponding chiller was installed in the system to condense the bulk of the water before it reaches the pump. This condenser can be valved into the system in series with the scroll vacuum pump or can be bypassed if not needed. The condenser cannot trap all the liberated free water, but is efficient at removing the majority of free water in the system. The condenser is only used during the first phase of a Cold Vacuum Drying (CVD) test for a single fuel element. The condenser was custom fabricated specifically for this system. Detailed sketches and specifications for the condenser are given in Ritter et al. (1998).

For the present test, an MKS Baratron model 626 pressure transducer was added into the system to accurately measure and record the outlet pressure of the condenser. This transducer was coupled to an MKS model PDR-C-2C two-channel power supply/readout unit.

### **2.2.3 Piping, Valves, and Filters**

The vacuum pumping system connects the system components through various valves, fittings, and piping. A simplified piping schematic for the system is shown in Figure 2.3. This schematic shows the basic flow path of gases through the system that was used for this test, along with the relative locations of the major components, valves, and instruments. Detailed system piping diagrams are provided in Ritter et al. (1998), along with approximate lengths for the piping lines. As seen in Figure 2.3, there are numerous valves in the system that are used to direct the flow to and from the various components. Most of the valves in the system are ball valves and range from 1/4 in. to 1/2 in. nominal size. The system piping is constructed of thin wall tubing (1/4 in. to 1/2 in. OD) and is typically connected using simple Swagelok fittings (tees, elbows, unions, etc.). Ports for gas sampling/analysis and monitoring of system pressure, temperature, and humidity are also provided at key locations in the system piping. Special fittings and pipe-threaded fittings are used in some locations for connecting piping to the process instruments.

Particulate filters are installed in the system on both the inlet and outlet to the retort to help prevent the spread of contamination to the system piping on the outside of the hot cell. These filters are constructed of a microporous fiberglass media in a stainless steel housing. They are 99.9% efficient for particulates that are 0.2 microns and larger in size. Two different size filters, manufactured by Matheson, are used in the system.

### **2.2.4 System Line Heaters**

All of the stainless steel tubing that carries gases into the furnace retort and resultant gases from the retort is heated to about 75°C to ensure condensable water vapor remains in the gas phase. Simple heat “cords” capable of being wrapped upon each other (as required at tees, elbows, and other connections)

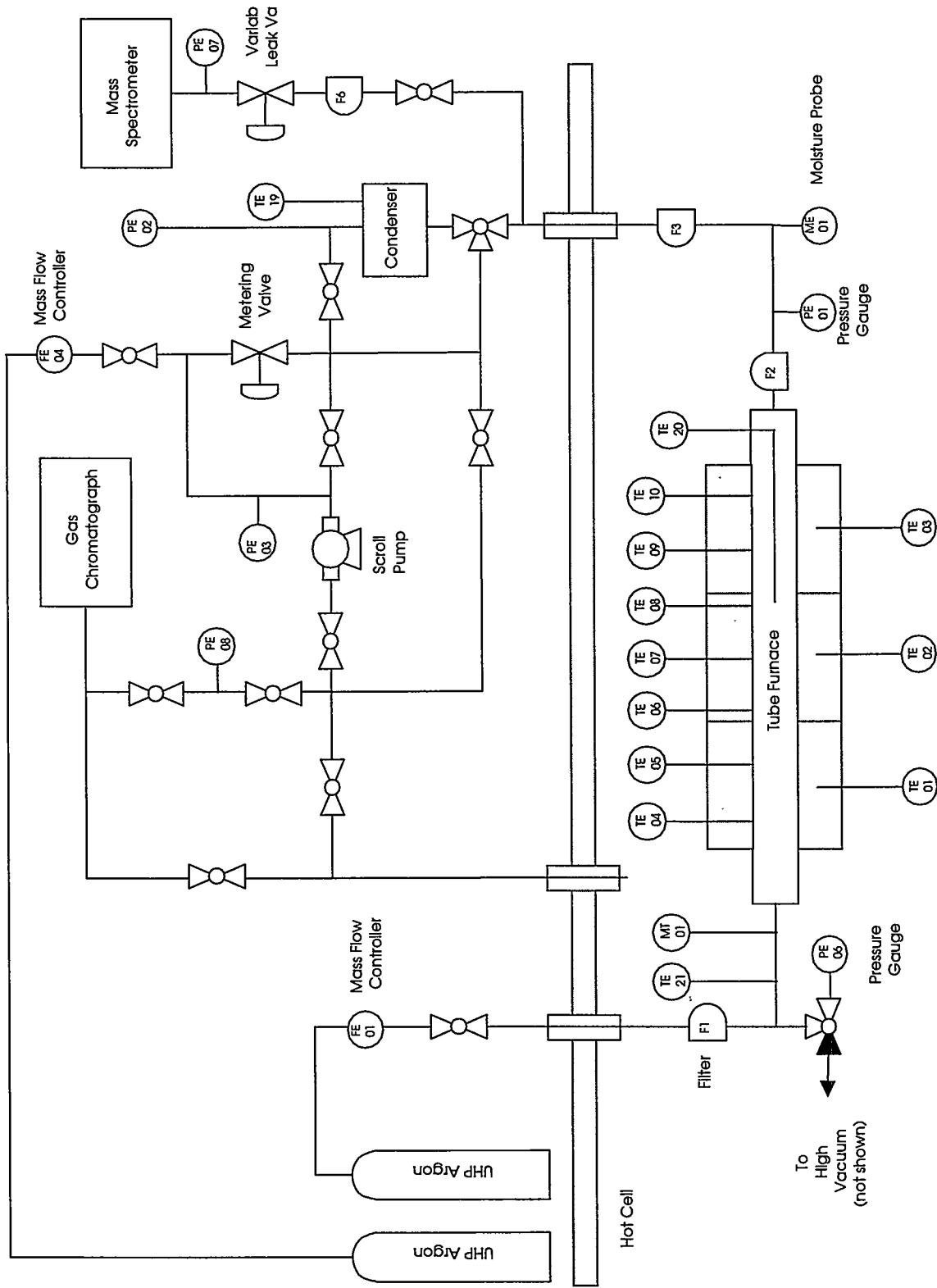


Figure 2.3. Generalized View of Test System

were found to be a good heating method for this system. The heating cords are controlled by simple proportional controllers. Type-K thermocouples are installed on each heated line so the DACS can be used to monitor and record temperature.

### **2.3 Process Heating System**

The whole element furnace is a 4-ft-long, resistively heated, clam-shell furnace. The furnace, a Series 3210 supplied by Applied Test Systems (ATS), has a temperature rating of 900°C and total heating capacity of 13,800 W. The internal dimensions are 5 in. ID by 45 in. long. The furnace has three separate sets of heating elements that allow the heating to be controlled in zones; each zone is 15 in. long and supplies up to 4600 W heating. The zones can be controlled separately to establish a flat temperature profile within the furnace, even though heat is lost preferentially out the end with the retort entry flange. A heat reflector consisting of several thin Inconel plates is used to reduce heat loss from the flange end of the retort. The furnace controller is an ATS Series 3000, which consists of three programmable, self-tuning proportional with integral and derivative controllers. These controllers are also interfaced to the DACS, which is capable of providing limited input to the controllers as required.

The retort, an ATS Series 3910, is an Inconel tube fitted with a gas inlet tube at one end and a gasketed flange at the other. Of all high-temperature materials, Inconel series 600 was selected to reduce the amount of oxidation and water pickup by the retort and associated components. Experience has shown that stainless steel components were easily affected by corrosion, which could then affect test results. The body of the retort is fabricated from schedule 40 Inconel pipe (4.5 in. OD, 4.026 in. ID), and the inside length is about 44.5 in.

Seven type-K thermocouples are installed equidistant along one side of the retort and extend into the retort interior approximately 1/8 in. These thermocouples are used to monitor the retort temperature so that if a reaction with the fuel element occurs (which would locally raise the retort temperature), this event can be correlated with the approximate location on the fuel.

An Inconel sample/transfer boat is used to load the fuel element into the furnace. The boat is fabricated from an 11-gauge (0.120-in.-thick) Inconel 601 sheet, which is formed into a flattened u-shape. The boat has a weir and a swivel handle on each end. The weirs are used to keep free water or particulates contained in the boat as required.

### **2.4 Gas Supply/Distribution System**

The gas supply system and vacuum pumping system together are capable of controlling the fuel element environment to vacuum or moderate pressure conditions, and/or exposing the fuel element to a variety of gases or gas mixtures. The gas loop is typically operated as a single-pass system with no capability for recirculation. The gas supply system consists of gas bottles; mass flow controllers; piping; and valves for metering argon, air, or oxygen through the system. A bubbler is also available for adding water vapor to the process gas stream as required, but it was not used in these tests.

The gas supply system contains three Matheson mass flow controllers calibrated for argon, air, and oxygen. All gases are typically specified "ultra high purity" and are additionally filtered for water using molecular sieve columns. Argon is the principal inert gas used, as it is more dense than air; provides reasonable thermal conductivity; and requires simpler handling procedures than lighter gases such as helium. The argon purge gas is introduced into the retort through FE-01, which is a Matheson model 8272-0422 oxygen controller, recalibrated for argon gas at 0°C using a NIST-traceable bubble flow meter. The recalibration resulted in a flow rate range of 0 - 304 standard cubic centimeters per minute (sccm) argon. Air and oxygen are not currently used because any oxidative steps have been deleted from the current IPS for the SNF. The manufacturer's specifications for the air and oxygen controllers' flow rate ranges are 0 - 1000 sccm air and 0 - 10 sccm oxygen. If higher flow rates are desired, a new mass flow controller with a higher range could be procured and installed in the system.

## **2.5 Gas Analysis Instrumentation**

### **2.5.1 Balzers Omnistar Mass Spectrometer**

The Balzers Omnistar MS is a compact, computer-controlled, quadrupole MS capable of scanning to 300 amu. The unit is capable of monitoring up to 64 components within a gas stream with a nominal detection limit of less than 1 ppm for most gases other than hydrogen. The MS was used to monitor hydrogen, nitrogen (for air in-leakage), krypton, xenon, and other elements during the test.

The MS was modified as a result of early system testing and calibration to improve the time response to small changes in hydrogen pressure. Before testing, the MS was calibrated for hydrogen using mixtures of hydrogen and helium, and hydrogen and argon gas. The residence time of each gas could be measured in the quadrupole chamber, and it was observed that the hydrogen decay time was approximately four times as long as helium. This was not unexpected as turbomolecular pumps have a lower pumping efficiency for very light gases. In standard practice this is acceptable, but for these tests, where determining hydrogen could be very important, steps were taken to improve the hydrogen decay time. The MS vacuum system was modified by adding a stainless steel flanged tee, a gate valve, and a room-temperature hydrogen getter downstream from the quadrupole. The getter was an SAES type 50-ST707. Under vacuum, the gate valve can be opened, exposing the getter to the system to help scavenge hydrogen from the system following analysis. This modification reduced the residence time of hydrogen in the system substantially and decreased the background level of hydrogen by about a factor of 2. The getter improved the system response to transient events that might result in the release of hydrogen.

A Granville-Phillips variable leak valve, series 203, was added to the gas sampling inlet of the MS to permit operation over a wide range of system pressures. Without the leak valve, system pressures above about 40 Torr produce too much flow through the MS capillary tube, which overwhelms the turbo pump used to pump down the MS vacuum chamber. Flow through the leak valve can be continuously varied from 0.4 l/s to  $10^{-11}$  l/s, which allows the MS inlet pressure to be controlled to any pressure desired, even if the system pressure varies dramatically. The pressure on the low-pressure side of the leak valve was measured and recorded by the DACS using a second MKS Baratron model 626 transducer (PE-07) combined with the MKS model PDR-C-2C two-channel power supply/readout unit above. This combination replaced the Cole-Parmer sensor that had both lower sensitivity and accuracy in this pressure

range and, thus, allowed for higher accuracy in the MS calibration. The inlet head pressure is divided by the pressure used for the calibration, and this factor is applied to the test data for calculating actual gas concentrations. Before the present test, the MS was calibrated at ~15 Torr head pressure with four certified gas standards consisting of  $10^2$ ,  $10^3$ ,  $10^4$ , and  $10^5$  parts per million by volume (ppmv) hydrogen in argon.

### **2.5.2 MTI M200 Gas Chromatograph**

The MTI M200 Gas Chromatograph is a high-speed GC that is used to monitor the quantities of hydrogen and other light gases in the furnace testing system gas loop. This instrument is interfaced with a laptop computer to record data. The GC is designed to operate at near-atmospheric pressure; thus, it may be configured in two different ways for measurement purposes. At system pressures near atmospheric, the GC is configured to sample directly from the gas loop ahead of the system vacuum pump. When the system is under vacuum, the GC is configured to sample from the exhaust side of the vacuum pump. The gas output from the pump is sufficiently compressed that the GC can sample and analyze this gas. The GC inlet pressure is measured using a Cole-Parmer pressure sensor (PE-08) and recorded by the DACS. No correction for the difference in the sample pressure and calibration pressure is applied, since both are ~760 Torr (1 atm). The GC was calibrated using the same four gas standards that were used for the MS calibration.

## **2.6 Process Instrumentation**

The furnace testing system contains several process instruments for monitoring moisture content, pressure, and temperature. The key instruments are as follows:

- Vaisala moisture monitor
- Panametrics moisture monitor
- MKS Baratron pressure transducers
- Cole-Parmer pressure transducer
- Type-K thermocouples.

### **2.6.1 Vaisala Moisture Monitor**

The Vaisala moisture monitor model HMP230 uses the HUMIDICAP sensor. This sensor is based on a capacitance change of a thin polymer film as the film absorbs water. The sensor has a nominal dew point range of  $-40^{\circ}\text{C}$  to  $100^{\circ}\text{C}$ . The probe tip is installed in the gas loop upstream of the furnace retort (see Figure 2.3). The sensor is designated as MT-01, and its integrated temperature sensor is designated as TT-01.



## 2.6.2 Panametrics Moisture Monitor

The Panametrics moisture monitor model MMS35 uses a solid electrochemical probe (model M2L) that measures moisture by measuring the characteristic capacitance of the probe as a function of the moisture in the gas phase. The sensor has a nominal dew point range of -110°C to 20°C. Previous testing indicated that contamination causes the probe to lose calibration and results in moisture readings that drift with time. To prevent contamination of the probe tip, the probe is installed in the gas loop downstream of two glass particulate filters. Further, the probes are changed following each test and surveyed for radioactive contamination. If no contamination is found, and the data correlate well with the data obtained from the MS, the readings are accepted.

A calibration verification procedure can be performed using calibrated water “leak” tubes. These tubes can be placed inside the furnace and, when heated, will establish a known water vapor pressure in the system. However, this procedure is time intensive; approximately 2 weeks are required to calibrate one probe over the range of moisture likely to be encountered in these tests. This procedure is only used if the moisture monitor results vary widely from the MS data.

Output of the moisture monitor is in dew point (DP) in degrees Celsius. For comparison with other test data, these dew point values were converted to water vapor pressure in Torr using the water and ice vapor pressure data shown in Table 2.1. Interpolation of the data was accomplished using a 6th-order polynomial fit to the log of the vapor pressure (VP) versus temperature data. The resulting conversion expression is as follows:

$$VP \text{ (Torr)} = \log^{-1}[C_1 \cdot DP^6 + C_2 \cdot DP^5 + C_3 \cdot DP^4 + C_4 \cdot DP^3 + C_5 \cdot DP^2 + C_6 \cdot DP + C_7] \quad (2.1)$$

where

- $C_1 = -6.7260E-12$
- $C_2 = -1.7250E-09$
- $C_3 = -1.7089E-07$
- $C_4 = -7.2618E-06$
- $C_5 = -2.9668E-04$
- $C_6 = +3.4414E-02$
- $C_7 = +6.5933E-01$

## 2.6.3 MKS Baratron Pressure Transducers

Two MKS Baratron model 690 calibrated pressure transducers coupled with MKS model 270 signal conditioners are used as the primary measurement for the overall system pressure. As shown in Figure 2.3, PE-01 measures the system pressure downstream of the retort outlet, whereas PE-06 measures the system pressure at the retort inlet. PE-01 indicates pressure in the range of 0.1 Torr to 10,000 Torr. The pressure range of PE-06 is 0.01 Torr to 1000 Torr. PE-06 was installed after the first two fuel element drying tests to provide more accurate measurements than PE-01 for low pressures. PE-06 is therefore considered the primary system pressure measurement. In addition, the 270 signal conditioner procured with PE-06 has a special capability to remotely zero the transducer, which provides more

**Table 2.1. Water and Ice Vapor Pressure Data Versus Temperature**

Dew Point (°C)	Vapor Pressure (VP)		
	(Pa) <sup>a</sup>	(Torr)	Log (Torr)
-80	5.500E-02	4.126E-04	-3.385E+00
-75	1.220E-01	9.151E-04	-3.039E+00
-70	2.610E-01	1.958E-03	-2.708E+00
-65	5.400E-01	4.051E-03	-2.392E+00
-60	1.080E+00	8.101E-03	-2.091E+00
-55	2.093E+00	1.570E-02	-1.804E+00
-50	3.936E+00	2.952E-02	-1.530E+00
-45	7.202E+00	5.402E-02	-1.267E+00
-40	1.284E+01	9.631E-02	-1.016E+00
-35	2.235E+01	1.676E-01	-7.756E-01
-30	3.801E+01	2.851E-01	-5.450E-01
-25	6.329E+01	4.747E-01	-3.235E-01
-20	1.033E+02	7.746E-01	-1.109E-01
-15	1.653E+02	1.240E+00	9.339E-02
-10	2.599E+02	1.950E+00	2.899E-01
-5	4.018E+02	3.014E+00	4.791E-01
0	6.113E+02	4.585E+00	6.614E-01
10	1.228E+03	9.212E+00	9.644E-01

(a) CRC Press. 1997. *Handbook of Chemistry & Physics*, 78<sup>th</sup> edition.

accurate pressure measurements below 1 Torr. Two additional MKS Baratron units were incorporated into the system for the present test; one to monitor the MS input pressure (see Section 2.5.1), and a second to monitor the input pressure to the scroll pump.

An auxiliary high vacuum turbo pump is used to evacuate the inlet to PE-06 to well below  $10^{-4}$  Torr so that the transducer can be accurately re-zeroed. The 270 signal conditioner used with PE-01 does not have a remote zeroing capability. Both signal conditioners have analog outputs that are interfaced to the DACS so that system pressure is continuously recorded.

#### 2.6.4 Cole-Parmer Pressure Transducer

A Cole-Parmer model H-68801-53 diaphragm-type, calibrated pressure transducer is installed on the GC sample line as indicated by PE-08 in Figure 2.3. This pressure measurement is used to normalize the GC data so that actual gas concentrations in the system can be calculated from the relative concentrations measured. This sensor has a range of 0 to 1500 Torr with a resolution of 0.1 Torr and an accuracy of  $\pm 1\%$  or  $\pm 1$  Torr, whichever is larger. The readout unit (model H-68801-03) has an analog output that is interfaced to the DACS.

### **2.6.5 Thermocouples**

Thermocouples provide a simple, reliable method for measuring system temperatures. As shown in Figure 2.3, over 20 thermocouples are installed at various locations in the system to provide key temperature measurements. The retort temperatures are of primary importance, and these temperatures are measured by thermocouples TE-04 through TE-10, which are positioned equidistant along the length of the retort. Other key temperature measurements include the retort center temperature (TE-20, which is a 30-in.-long thermocouple installed through the outlet end of the retort); retort inlet temperature (TE-21); condenser gas temperature (TE-19); and the condenser coolant temperature (TE-22). Thermocouples TE-11 through TE-17 are used for controlling the temperature of the heated lines. All thermocouple readings are continuously recorded using the DACS.

### **2.7 Data Acquisition and Control System**

The DACS monitors system parameters and controls the furnace and the safety argon system. The DACS consists of a Hewlett Packard (HP) 3497A data acquisition/control unit, and an IBM-compatible computer. A National Instruments general purpose interface bus card, installed in the IBM-compatible computer, is used to communicate with the HP 3497A. The computer communicates with the furnace temperature controllers over serial port 0 using an RS-232/RS-485 converter. The DACS uses National Instruments LabView for Windows as the control software.

The DACS is designed to measure critical system parameters during fuel conditioning tests, including temperatures, pressures, flow rates, and moisture level. The measured parameters are converted to engineering units, displayed on the computer screen, and stored to disk at user-defined intervals. The data files are stored in a tab-delimited format to allow importing into a standard spreadsheet or plotting program. A plotting screen also allows for plotting of up to six parameters at a time.

Limited control of the furnace can be performed with the DACS. Each of the three furnace zone temperatures can be remotely set by the DACS. In addition, the DACS allows the operator to start and stop the furnace and select one of four temperature profiles that are pre-programmed in the furnace temperature controllers. Note that these profiles must be programmed manually in the furnace controllers before using the DACS to select them.

## 3.0 Vacuum Drying Testing of Furnace System

The drying test was performed in accordance with Test Procedure, *Wet/Dry Run Testing of G-Cell Furnace System in Preparation for Run #8*, 3M-TWD-PTL-013, Revision 0. This document is located in the PNNL permanent project records for this test.

The testing consisted of three parts (discussed in this section):

- preparation and loading of the empty fuel element sample boat into the furnace
- drying the empty sample boat and furnace system using a combination of Cold Vacuum Drying (CVD) and Hot Vacuum Drying (HVD) processes
- cooldown and unloading of the furnace.

### 3.1 Initial Conditions

Ten milliliters of water were added to the sample boat before the start of the test. The test conditions used were otherwise the same as those used for the subsequent drying test on Element 6513U (Run 8).

### 3.2 System Drying

The empty fuel element boat and furnace system was subjected to cold and hot vacuum drying. The drying process was conducted in six phases:

1. Cold Vacuum Drying
2. Pressure Rise Test
3. Hot Vacuum Drying (first step)
4. Hot Vacuum Drying (second step)
5. Hot Vacuum Drying (third step)
6. Cooldown and Post-Test Pressure Rise Test.

The nominal design conditions used for these test phases are summarized in Table 3.1. Each phase is discussed below.

**Table 3.1. Summary of Nominal Test Design Conditions**

Test Segment	Nominal Test Condition <sup>(a)</sup>
<b>A. Cold Vacuum Drying</b> System Configuration  Test Temperature, °C Atmosphere Pressure, Torr Gas Flow Rate, cc/min Gas Species Monitored Duration, hr	Pump on, <sup>(b)</sup> argon gas flow during initial condenser pumpdown phase  50 Vacuum <5 0 except during initial condenser phase H <sub>2</sub> , H <sub>2</sub> O, N <sub>2</sub> , O <sub>2</sub> , CO <sub>2</sub> , Ar, Kr, Xe CVD is conducted until the total pressure in the retort falls below 0.5 Torr.
<b>B. Pressure Rise Test</b> System Configuration Test Temperature, °C Atmosphere Initial Pressure, Torr Gas Flow Rate, cc/min Pressure Rise (acceptable level, Torr) Duration, hr	Test Chamber Isolated  50 Vacuum <5 0 <0.5 1
<b>C. Hot Vacuum Drying (Step 1)</b> System Configuration Test Temperature Range, °C Atmosphere Pressure, Torr Gas Flow Rate, cc/min Gas Species Monitored Duration, hr	Pump on, <sup>(b)</sup> argon gas flow 75 Vacuum, Ar background 15 300 H <sub>2</sub> , H <sub>2</sub> O, N <sub>2</sub> , O <sub>2</sub> , CO <sub>2</sub> , Ar, Kr, Xe 24
<b>D. Hot Vacuum Drying (Step 2)</b> System Configuration Test Temperature Range, °C Temperature Ramp Rate, °C/hr Atmosphere Pressure, Torr Gas Flow Rate, cc/min Gas Species Monitored Duration, hr	Pump on, <sup>(b)</sup> argon gas flow 75 to 400 10 Vacuum, Ar background 15 300 H <sub>2</sub> , H <sub>2</sub> O, N <sub>2</sub> , O <sub>2</sub> , CO <sub>2</sub> , Ar, Kr, Xe 35

Table 3.1. (contd)

Test Segment	Nominal Test Condition <sup>(a)</sup>
<b>E. Hot Vacuum Drying (Step 3)</b>	
System Configuration	Pump on, <sup>(b)</sup> argon gas flow
Test Temperature, °C	400
Atmosphere	Vacuum, Ar background
Pressure, Torr	15
Gas Flow Rate, cc/min	300
Gas Species Monitored	H <sub>2</sub> , H <sub>2</sub> O, N <sub>2</sub> , O <sub>2</sub> , CO <sub>2</sub> , Ar, Kr, Xe
Duration, hr	10
<b>F. Cooldown</b>	
System Configuration	Pump on, <sup>(b)</sup> argon gas flow
Test Temperature, °C	400 to 50
Atmosphere	Vacuum
Initial Pressure, Torr	15
Gas Flow Rate, cc/min	300
Gas Species Monitored	H <sub>2</sub> , H <sub>2</sub> O, N <sub>2</sub> , O <sub>2</sub> , CO <sub>2</sub> , Ar, Kr, Xe
Duration, hour	~100
<b>G. Pressure Rise Test</b>	
System Configuration	Test Chamber Isolated
Test Temperature, °C	50
Atmosphere	Vacuum
Initial Pressure, Torr	<5
Gas Flow Rate, cc/min	0
Duration, hour	1
(a) Nominal test design conditions. Actual values are given in the text.	
(b) Vacuum pump was throttled during the drying test.	

### 3.2.1 Cold Vacuum Drying

The furnace was first purged with argon to remove as much air as possible. The furnace was then isolated and the furnace temperature increased to approximately 50°C and allowed to stabilize. After stabilization, argon flow was re-established; the system vacuum pump was turned on (in a throttled mode); and the system water condenser valved in. When the system pressure became lower than the condenser could extract, the condenser was valved out of the gas loop and the argon flow stopped. The remainder of the CVD was conducted with the throttled vacuum pump. CVD was conducted at an ultimate pressure of ~0.3 Torr for ~19 hr. The purpose of the CVD portion of the test was to determine if CVD is successful in removing the majority of the free water from the system in a reasonable length of time.

### **3.2.2 Pressure Rise Test**

The Pressure Rise Test involved isolating the system and measuring any pressure increase while at CVD pressure and temperature conditions. The purpose of the Pressure Rise Test was to determine the effectiveness of the preceding CVD process. This test was conducted by valving the vacuum pump out of the gas loop and closing the exhaust valves. The condition for acceptance of this portion of the test was a total system pressure rise of less than 0.5 Torr in a 1-hr time period. If this condition was not met, the system was re-opened to the vacuum pump and the Pressure Rise Test repeated.

### **3.2.3 Hot Vacuum Drying, Step 1**

Following completion of the Pressure Rise Test, the vacuum pump was re-opened to the system retort; argon gas flow was established at a rate of ~304 cc/min; and the retort temperature was increased to ~75°C. This condition was held for a period of ~25 hr. This portion of the test can be used to obtain isothermal hydrogen and water release data for assessing oxidation of the fuel at low temperatures.

### **3.2.4 Hot Vacuum Drying, Step 2**

The second step of the HVD process involved raising the temperature of the retort from ~75°C to ~400°C at a carefully controlled rate (10°C/hr) while maintaining the same argon flow and pressure conditions. With this process, any release of gas species during this temperature rise could be assigned to a specific temperature. The second step of HVD was conducted for about 34 hr.

### **3.2.5 Hot Vacuum Drying, Step 3**

The final step of the HVD process involved holding the temperature of the retort at ~400°C while again maintaining the same argon flow and pressure conditions as in steps 1 and 2. This step will yield isothermal release data for any remaining hydrated species on a fuel element and for oxidation of uranium by any remaining water. This final step of the HVD process was conducted for about 8 hr.

### **3.2.6 System Cooldown and Post-Test Pressure Rise Test**

Following completion of the final HVD step, the system retort was allowed to cool to ~50°C while maintaining the same vacuum and flow conditions, and then another Pressure Rise Test was conducted to determine the baseline in-leakage rate of air into the retort from the cell environment. Knowing this rate is important to allow for correction of the system and moisture pressure increase rates determined in the initial post-CVD Pressure Rise Test. Since the conditions for the post-HVD test are identical to those used for the initial test, the assumption is made that the air in-leakage rate should be nearly the same as well.

### 3.3 Calculation of Water and Hydrogen Inventories

Assuming ideal gas behavior of the water vapor, total water inventory ( $m$ ) in the system during those portions of the test conducted with argon flowing into the retort can be approximated from the measured water vapor pressure and the argon gas flow as follows:

$$\frac{dm}{dt} = \frac{M}{V_0} \cdot \frac{P_w}{(P_t - P_w)} \cdot \frac{dV}{dt} \quad (3.1)$$

where  $dm/dt$  is the rate of water removal in grams per minute,  $M$  is the molecular mass of water in grams per mole,  $dV/dt$  is the flow rate in liters per minute (at the calibration temperature of  $0^\circ\text{C}$ ),  $V_0$  is the molar volume of gas at  $0^\circ\text{C}$  and 1 atmosphere in liters per mole,  $P_w$  is the partial pressure of water vapor in Torr, and  $P_t$  is the total pressure in Torr. The total amount of water released is given by integrating the rate data over time.

The hydrogen inventory may be calculated in a similar fashion with the  $[P_w/(P_t - P_w)]$  expression in the above equation replaced with the measured atom fraction of hydrogen. For the purposes of this report, all hydrogen data are plotted in Torr-l rather than grams. At the calibration conditions of the argon flow controller, 1 Torr-l is equivalent to approximately 0.12 mg of hydrogen.

The assumptions made in estimating the water and hydrogen values are:

- The flow into the retort is approximately equal to the flow out (i.e., contributions to the flow from other gas species such as hydrogen are neglected).
- The argon mass flow is referenced to  $0^\circ\text{C}$  (as determined from the calibration of the flow gauges).
- The sample gas is at the same temperature as the calibration gas (GC and MS measurements).



## 4.0 Experimental Results

In the following sections, the experimental data collected during the dry-run test are expanded and plotted for each segment. Summary results from the test are shown in Figure 4.1. This figure shows the system moisture level response to the pressure changes and the retort tube temperatures during the test. Time intervals for the various test segments are shown in the upper section of the plot and also outlined in Table 4.1. The temperatures shown in Figure 4.1 were recorded from one of seven thermocouples (TE-07) on the system located near the center of the retort. The pressure data were taken from the 0 to 1000 Torr Baratron sensor (PE-06) located upstream of the retort.

### 4.1 Cold Vacuum Drying

The water release from the CVD portion of the test is shown in Figure 4.2. The baseline moisture partial pressure in the system before heating was ~6 Torr at a retort temperature of ~22°C. Total system pressure was ~743 Torr, with no argon gas flow. After heating to ~50°C, the moisture pressure and system pressure stabilized at ~5 Torr and ~822 Torr, respectively. Assuming ideal gas behavior, the pressure after heating was approximately 8 Torr higher than expected. This excess pressure has been observed in all previous tests, except for the first dry-run, and may be due to gases evolved during the heatup, such as hydrogen from moisture reactions with the empty retort, and gases dissolved in the free water. Another explanation for the calculated pressure difference is that the average retort temperature was somewhat greater than 50°C.

The CVD phase started at an elapsed time (ET) of 253 min. Figure 4.2 shows that the moisture pressure rose almost immediately to ~9 Torr, followed by a relatively steady decrease over the remainder of CVD. A small jump in the moisture pressure at an ET of 299 min coincides with isolation of the condenser and cessation of argon gas flow. Pumping was continued by the throttled vacuum pump alone. Small drops in the moisture pressure at ET 311 and 468 min coincide with small jumps in the retort pressure read by both PE-01 and PE-06. The first pressure jump was caused by the opening of the MS leak valve for the start of MS scans. The second was likely due to outgassing of some system component. By the end of CVD (ET = 1391), the moisture pressure had dropped to ~0.1 Torr, and the total pressure had dropped to ~0.25 Torr.

Approximately 3 ml of water were observed in the condenser during the CVD phase. Because of the design of the condenser, however, it is possible that the observed water is an underestimation of the total water collected. Calculated water removal during the time period when the condenser was open under argon flow yielded a value of ~1.4 g, somewhat lower than the water observed in the condenser. Approximately 10 ml of water were added at the start of the test. The reason for the under-recovery of water in the condenser may be due to hang-up of water in colder sections of the system, particularly the particulate filters. Review of previous drying test data shows good correlation of fractional water recovery versus duration of the condenser pumpdown phase. Run 7 (Element 2660M), which had a much longer condenser phase, showed significantly higher fractional water recovery.

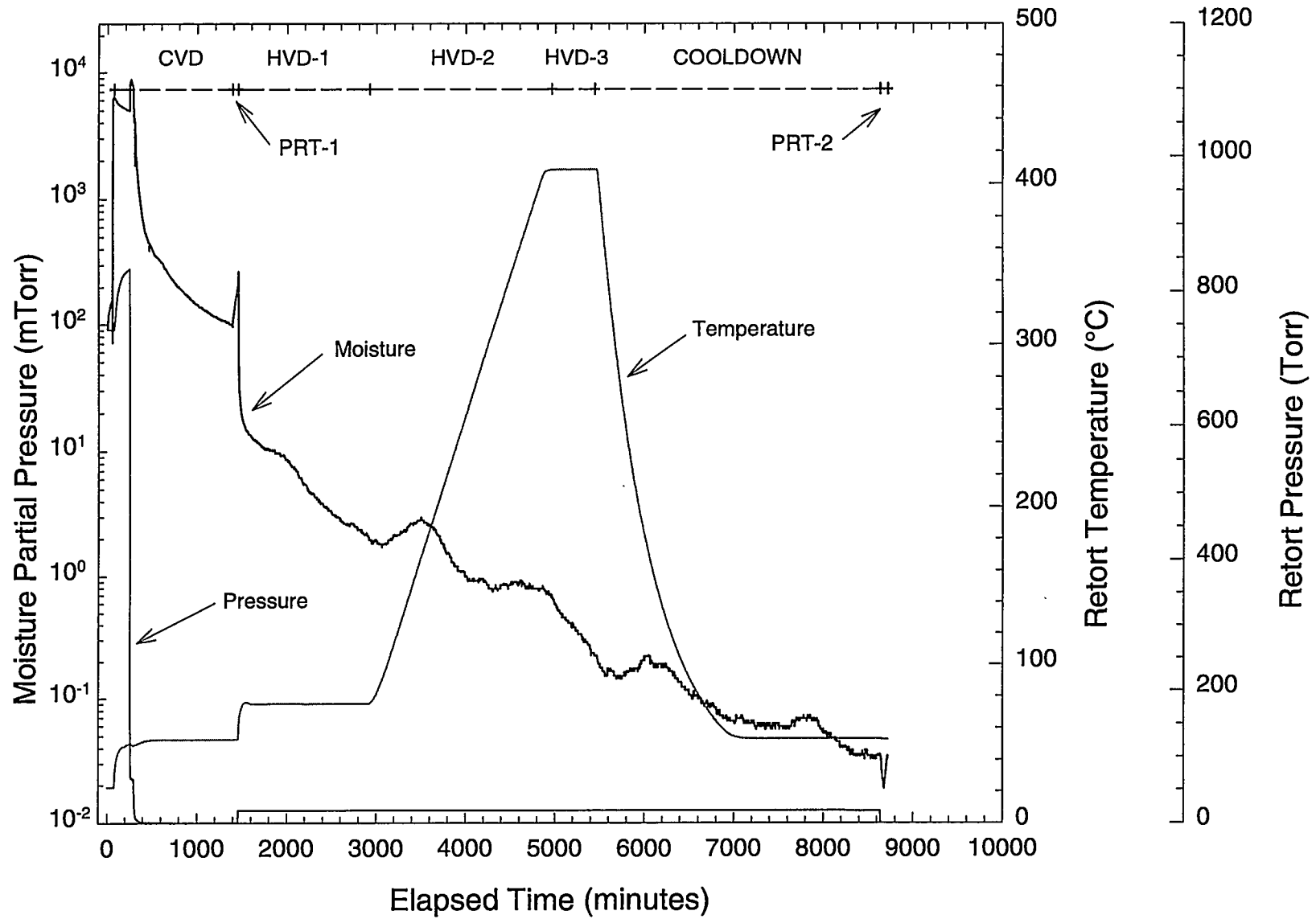


Figure 4.1. Spent Fuel Drying System Test Results, Summary Plot

**Table 4.1. Dry-Run Time Line**

<b>Activity</b>	<b>Date/Time</b>	<b>Elapsed Time (min)</b>
<b>Start of Test</b>		
Heat furnace to ~50°C	05/12/98 10:38	74
<b>Cold Vacuum Drying Test</b>		
Open pump <sup>(a)</sup> and condenser (initial), start argon flow	05/12/98 13:27	253
Open pump, close condenser (final), stop argon flow	05/12/98 14:23	299
<b>Pressure Rise Test</b>		
Close pump (isolate furnace)	05/13/98 08:36	1392
Open pump valve	05/13/98 09:38	1454
<b>Hot Vacuum Drying Test (Step 1)</b>		
Start argon flow (~300 sccm), raise furnace temperature to ~75°C and hold	05/13/98 09:39	1455
<b>Hot Vacuum Drying Test (Step 2)</b>		
Raise furnace temperature to ~400°C @ 10°C/min	05/14/98 10:09	2925
<b>Hot Vacuum Drying Test (Step 3)</b>		
Hold furnace temperature at ~400°C	05/15/98 20:09	4965
<b>System Cooldown</b>		
Reduce temperature of retort to ~50°C, maintain argon flow	06/16/98 04:09	5445
<b>Post-Test Pressure Rise Test</b>		
Turn off argon flow, and close pump valve (isolate furnace)	05/18/98 09:18	8634
Turn off furnace heaters, end test	05/18/98 10:44	8720
(a) The vacuum pump was throttled for the drying test.		

During the condenser pump-out phase of CVD, the partial pressure of hydrogen in the retort decreased from ~3 mTorr to ~0.02 mTorr, and correlated reasonably well with the water partial pressure during this time. During fuel element testing (e.g., Run 7), observed hydrogen partial pressures are generally three to four orders of magnitude higher, likely resulting from reactions between water vapor and uranium in the fuel through the reaction



## 4.2 Pressure Rise Tests

The results of the two pressure rise phases of the drying test (post-CVD and post-HVD) are shown in Figures 4.3 and 4.4. As discussed earlier, the purpose of the post-HVD test was to determine as best as possible the ambient air in-leakage rate into the system as it had been configured for the drying test. While under vacuum conditions, with no argon flow, any air in-leakage will contribute to the data signals observed for the various process gases measured during the test, particularly water and hydrogen. The data plotted for the total pressure are from the 0 to 1000 Torr Baratron sensor (PE-06) located upstream

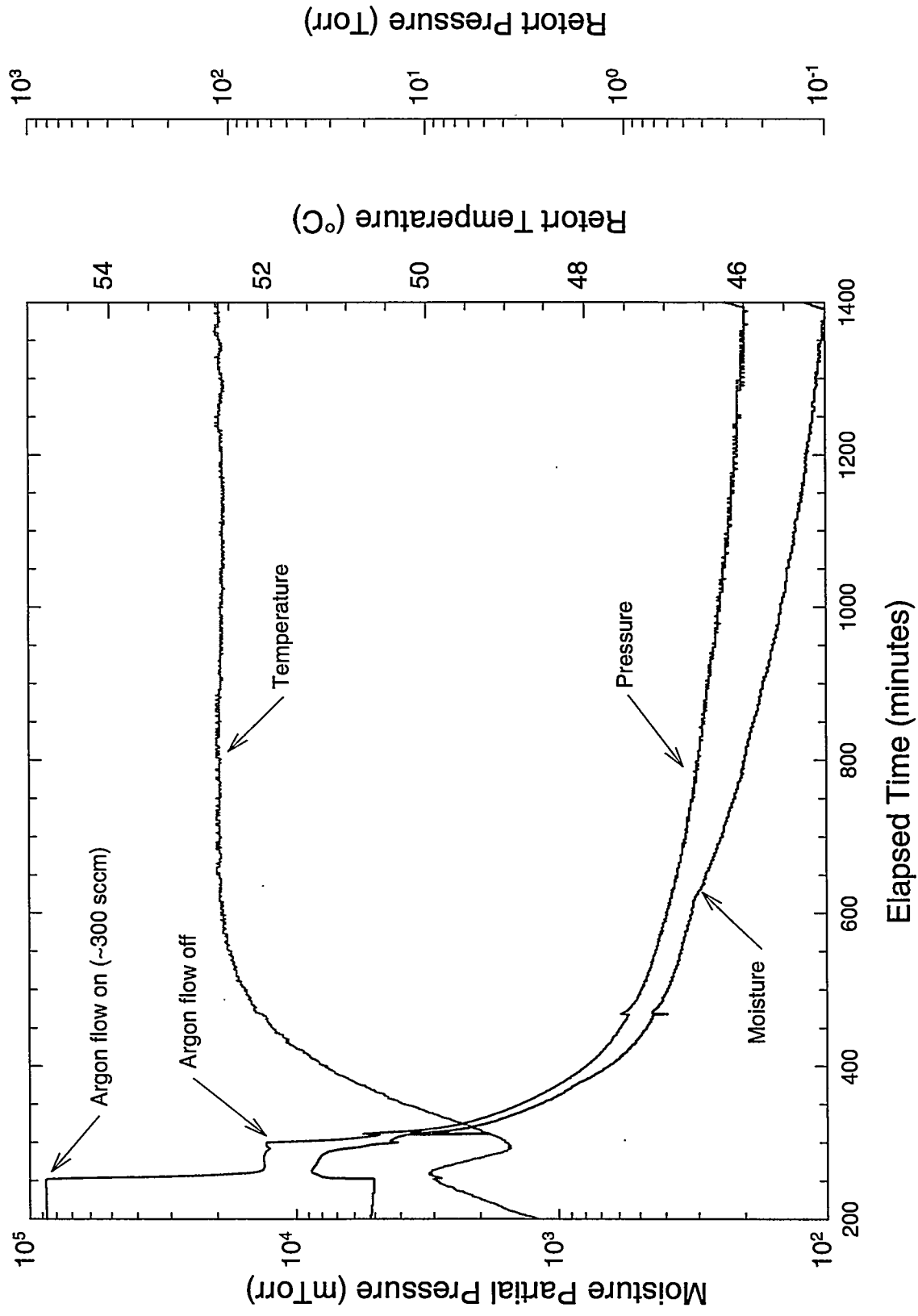


Figure 4.2. Spent Fuel Drying System Test Results, Cold Vacuum Drying

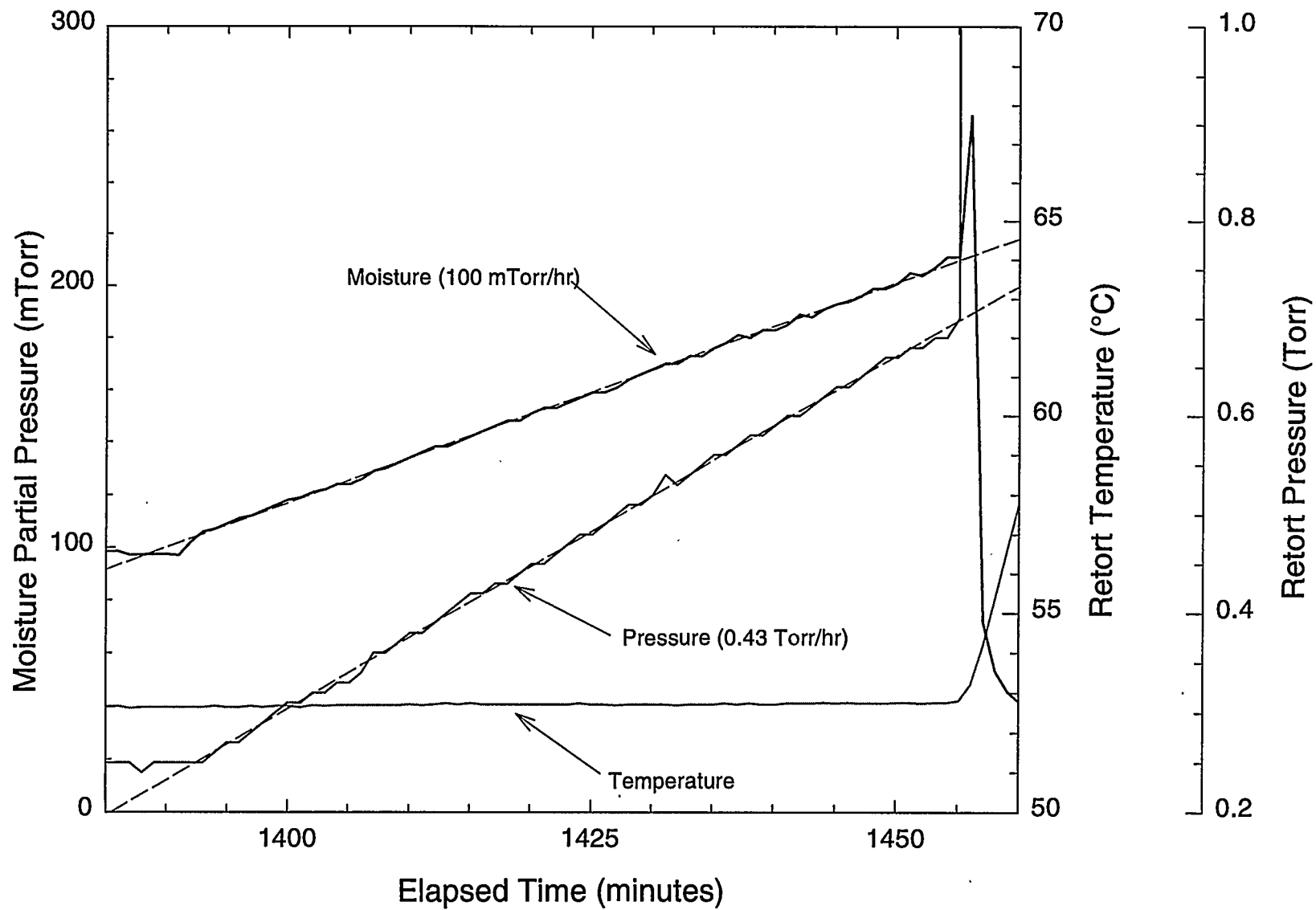


Figure 4.3. Spent Fuel Drying System Test Results, Post-CVD Pressure Rise Test

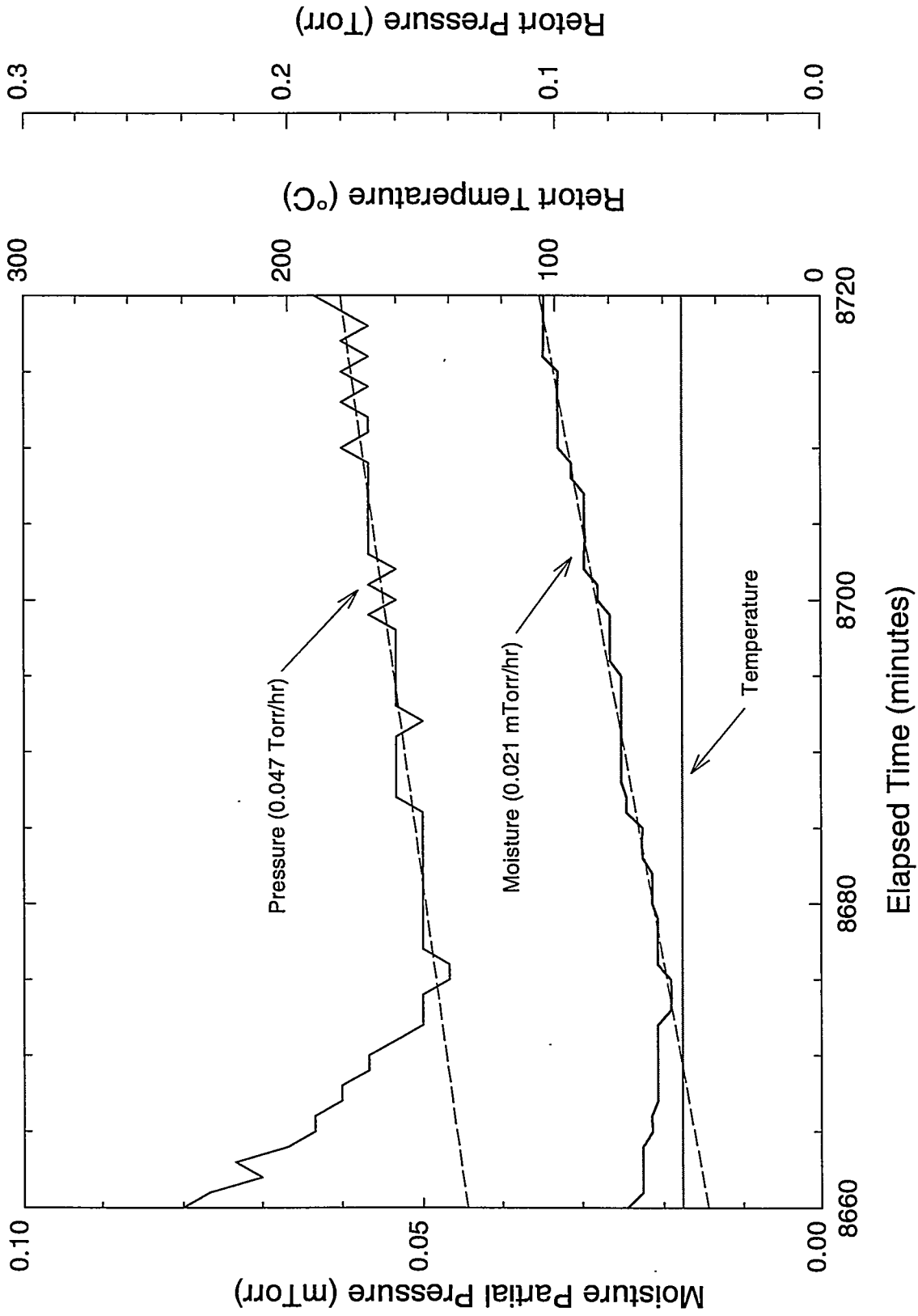


Figure 4.4. Spent Fuel Drying System Test Results, Post-HVD Pressure Rise Test

of the retort. This sensor has higher sensitivity and therefore lower noise than the 0 to 10,000 Torr Baratron (PE-01) located downstream of the retort. To calculate the total water mass removed from the retort, however, pressure data from the 0 to 10,000 Torr sensor were used, as this sensor is closer to the moisture sensor. Differences in the pressure indications of the two sensors are generally small; however, for the present test, there was some observed variation in the pressure indication of PE-01 during the latter phase of CVD. Since there was no argon flow during this period, this variation had no effect on any calculated water removal values.

The post-CVD Pressure Rise Test was conducted over an ET of 1392 min to 1454 min. Both the total pressure and the moisture pressure showed nearly linear pressure rises over the course of the test. Regression fits (dotted lines in the figure) yielded a total pressure rise rate of  $\sim 0.43$  Torr/hr (below the 0.5 Torr/hr criterion for the test), and a moisture pressure rise rate of  $\sim 0.10$  Torr/hr.

Assuming that the water vapor pressure increase is from water sources within the test system, and assuming ideal gas behavior of the water vapor, the rate of desorption of the water ( $dn/dt$ ) will be constant, given by:

$$\frac{dn}{dt} = \frac{V}{RT} \cdot \frac{dP}{dt} \quad (4.2)$$

where  $n$  is the number of moles of gas,  $V$  is the volume of the system ( $\sim 10,000 \text{ cm}^3$ ),  $R$  is the gas constant ( $82.06 \text{ cm}^3 \cdot \text{atm} / \text{g} \cdot \text{mol} \cdot \text{K}$ ),  $T$  is the temperature ( $\sim 326 \text{ K}$ ), and  $dP/dt$  is the rate of change in the pressure given by the slope of the regression line. The total amount of water released to the system during the Pressure Rise Test, given by the integral of the above equation, was  $\sim 1.0 \text{ mg}$ . Assuming a total surface area of  $\sim 6700 \text{ cm}^2$  for the system (total surface area of the retort, sample boat, and tubing), and  $10^{15}$  atoms per  $\text{cm}^2$  as the monolayer gas density on surfaces, approximately five monolayer equivalents of  $\text{H}_2\text{O}$  were evaporated.

The results of the post-HVD pressure rise measurements are shown in Figure 4.4. Again, both the total pressure and the moisture pressure showed essentially linear increases with time, however with significantly lower slopes than observed for the earlier post-CVD test. The total pressure rise has a regression slope of  $\sim 0.047$  Torr/hr, and the moisture pressure has a slope of  $\sim 0.000021$  Torr/hr. The rate of increase in the total pressure is similar to that observed in the previous three fuel element tests (Runs 5, 6, and 7).

The ratio of the water pressure rise to the total pressure is  $\sim 0.0004$ , somewhat lower than would be expected just from humidity alone in air in-leakage from the cell environment (air at  $20^\circ\text{C}$  and 25% relative humidity would yield a water pressure-to-total pressure ratio of  $\sim 0.007$ ). This has been observed in previous fuel element drying tests (e.g., Runs 4 and 5), and the proposed mechanism was that the vacuum drying of the fuel element at temperature (during CVD and HVD) resulted in the formation of hygroscopic species that "gettered" most of the moisture from either air in-leakage or moisture remaining on the element that would otherwise have been released. In this test, where no fuel element was present, it is assumed that most of the moisture from the air in-leakage was re-adsorbed on the "dry" walls of the furnace system.

Comparing the data from the two Pressure Rise Tests indicates that the total pressure rise observed in the initial post-CVD test was only partially caused by residual moisture and/or air in-leakage. Specifically, the difference between the total pressure rise and the moisture pressure rise for the post-CVD test ( $\sim 0.3$  Torr/hr) is significantly higher than the air in-leakage rate into the retort as measured in the post-HVD test ( $\sim 0.05$  Torr/hr). This suggests that other sources of gas are responsible for some of the observed total pressure rise in the post-CVD test, even with no fuel element present.

### 4.3 . Hot Vacuum Drying

The first segment of HVD, shown in Figure 4.5, includes the ramp and hold from  $\sim 50^{\circ}\text{C}$  to  $\sim 75^{\circ}\text{C}$  in flowing argon gas ( $\sim 304$  cc/min) under partial vacuum. HVD-1 occurred over an ET of 1455 min to 2924 min. The moisture pressure decreased steadily from  $\sim 200$  mTorr to  $\sim 2$  mTorr during the  $\sim 75^{\circ}\text{C}$  phase. Total system pressure was essentially constant over this first HVD phase at  $\sim 19$  Torr. Total water removed was  $\sim 0.2$  g.

The second HVD phase involved maintaining the same system conditions as in HVD-1, but raising the temperature slowly from  $\sim 75^{\circ}\text{C}$  to  $\sim 400^{\circ}\text{C}$  at a rate of  $10^{\circ}\text{C/hr}$ . HVD-2 occurred over an ET of 2925 min to 4964 min and is shown in Figure 4.6. During the temperature rise, the moisture pressure increased slightly, reaching a maximum value of  $\sim 30$  mTorr at  $\sim 170^{\circ}\text{C}$  before dropping and leveling off at  $\sim 0.8$  mTorr at a temperature of  $\sim 300^{\circ}\text{C}$ . Total water removed during the second phase of HVD was  $\sim 0.05$  g, about one quarter of that removed during the first phase. Total system pressure remained constant at  $\sim 19$  Torr.

The third phase of HVD is shown in the left-hand side of Figure 4.7 (ET of 4965 min to 5444 min) and covered the temperature hold period at  $\sim 400^{\circ}\text{C}$ . This period is characterized by a steady decrease in the moisture pressure from  $\sim 0.8$  mTorr to  $\sim 0.2$  mTorr. Total water removed was  $\sim 4$  mg.

Following the final HVD phase, the system was allowed to cool to  $\sim 50^{\circ}\text{C}$  in preparation for the post-test Pressure Rise Test discussed above. Water removed during the system cooldown was  $\sim 6$  mg. Total system pressure remained constant at  $\sim 19$  Torr during HVD-3 and cooldown.

### 4.4 Gas Chromatograph Measurements

The GC was used to measure hydrogen in the sample gas during a portion of the CVD step and during the HVD step (when argon was flowing through the system). Hydrogen signals during CVD and HVD were very near the detection limit for the GC instrument. Hydrogen data collected during the condenser pumpdown phase of CVD are shown in Figure 4.8. Hydrogen values during this phase generally followed the moisture signal, starting at  $\sim 1$  mTorr·l/min and steadily dropping to  $\sim 0.1$  mTorr·l/min. Total hydrogen released during this period was  $\sim 0.1$  Torr·l ( $\sim 0.001$  mg).

Measured hydrogen release during the HVD segments of the drying test is shown in Figure 4.9. Hydrogen signals showed a slow increase over HVD from about  $0.3$  mTorr·l/min to about  $8$  mTorr·l/min.



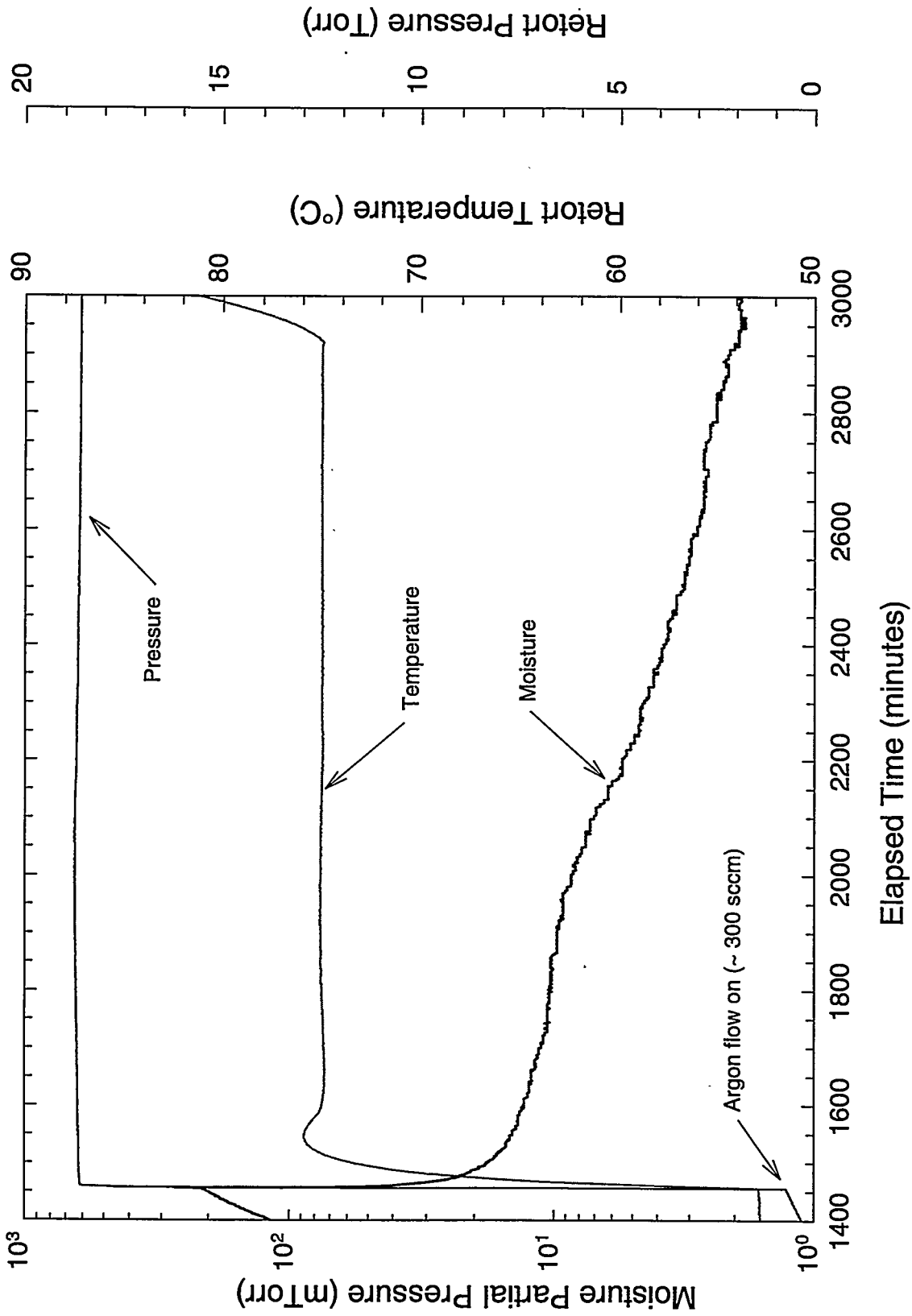


Figure 4.5. Spent Fuel Drying System Test Results, Hot Vacuum Drying – Step 1

4.10

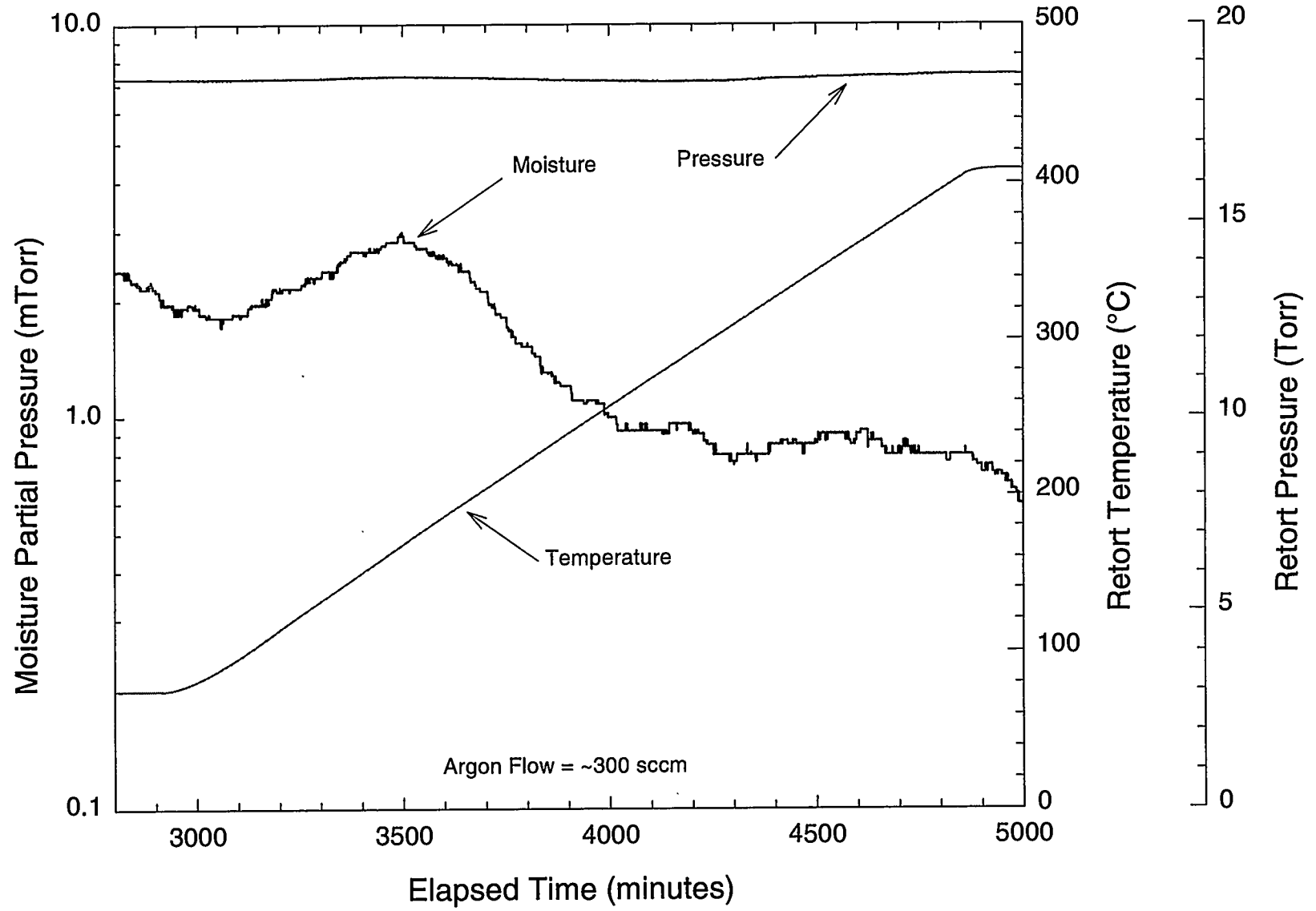


Figure 4.6. Spent Fuel Drying System Test Results, Hot Vacuum Drying – Step 2

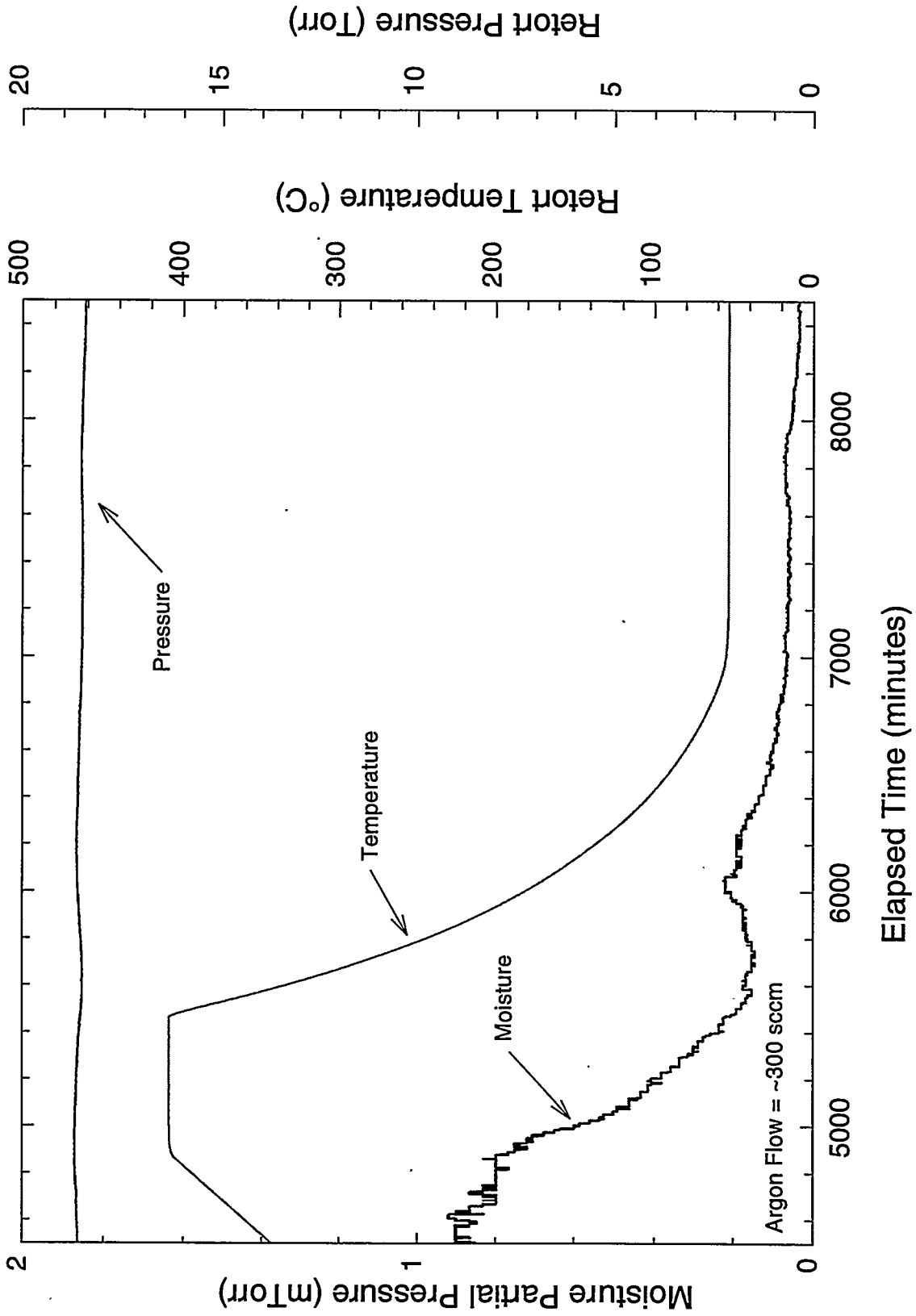


Figure 4.7. Spent Fuel Drying System Test Results, Hot Vacuum Drying – Step 3

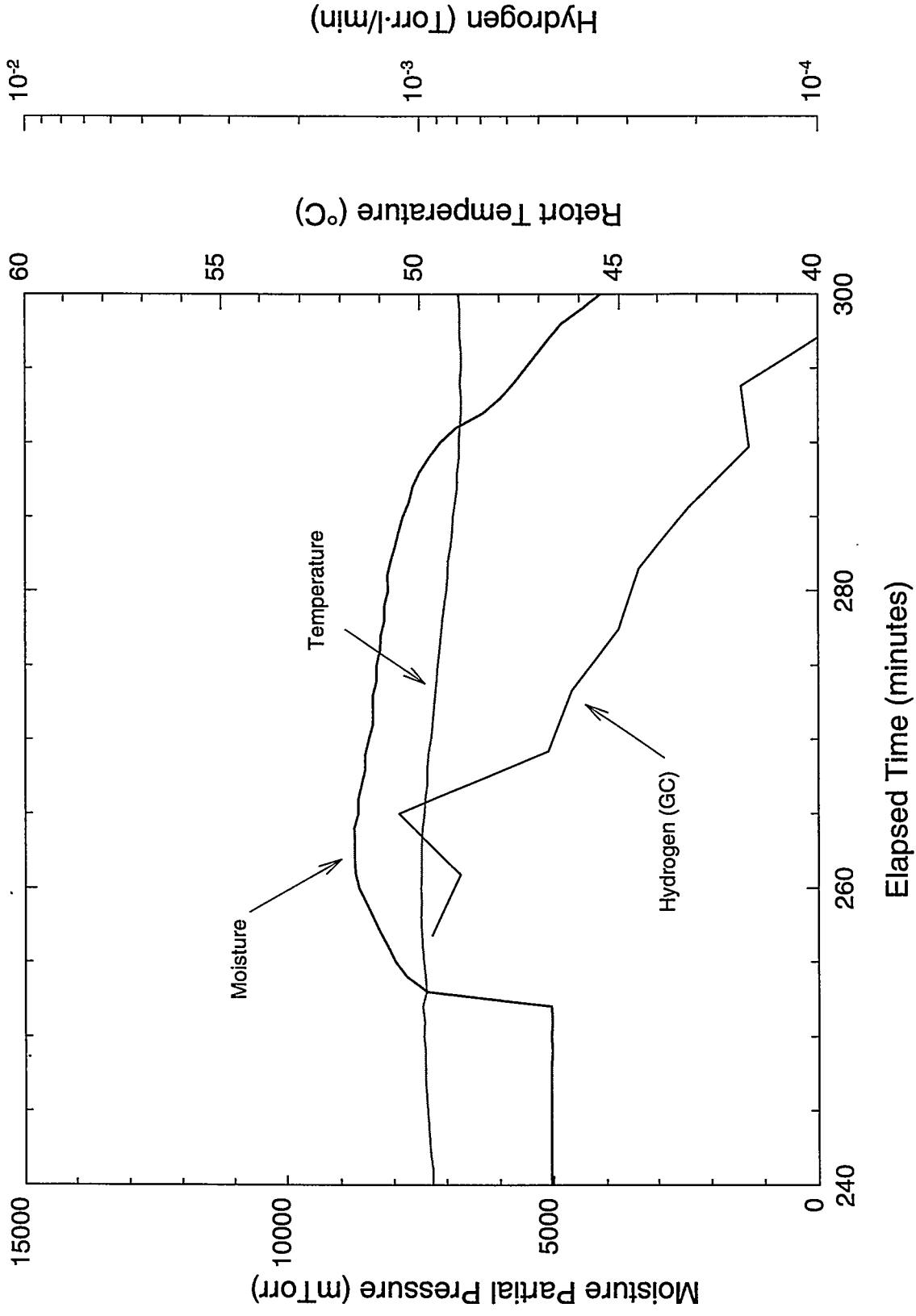


Figure 4.8. Spent Fuel Drying System Test Results, Hydrogen Release During CVD

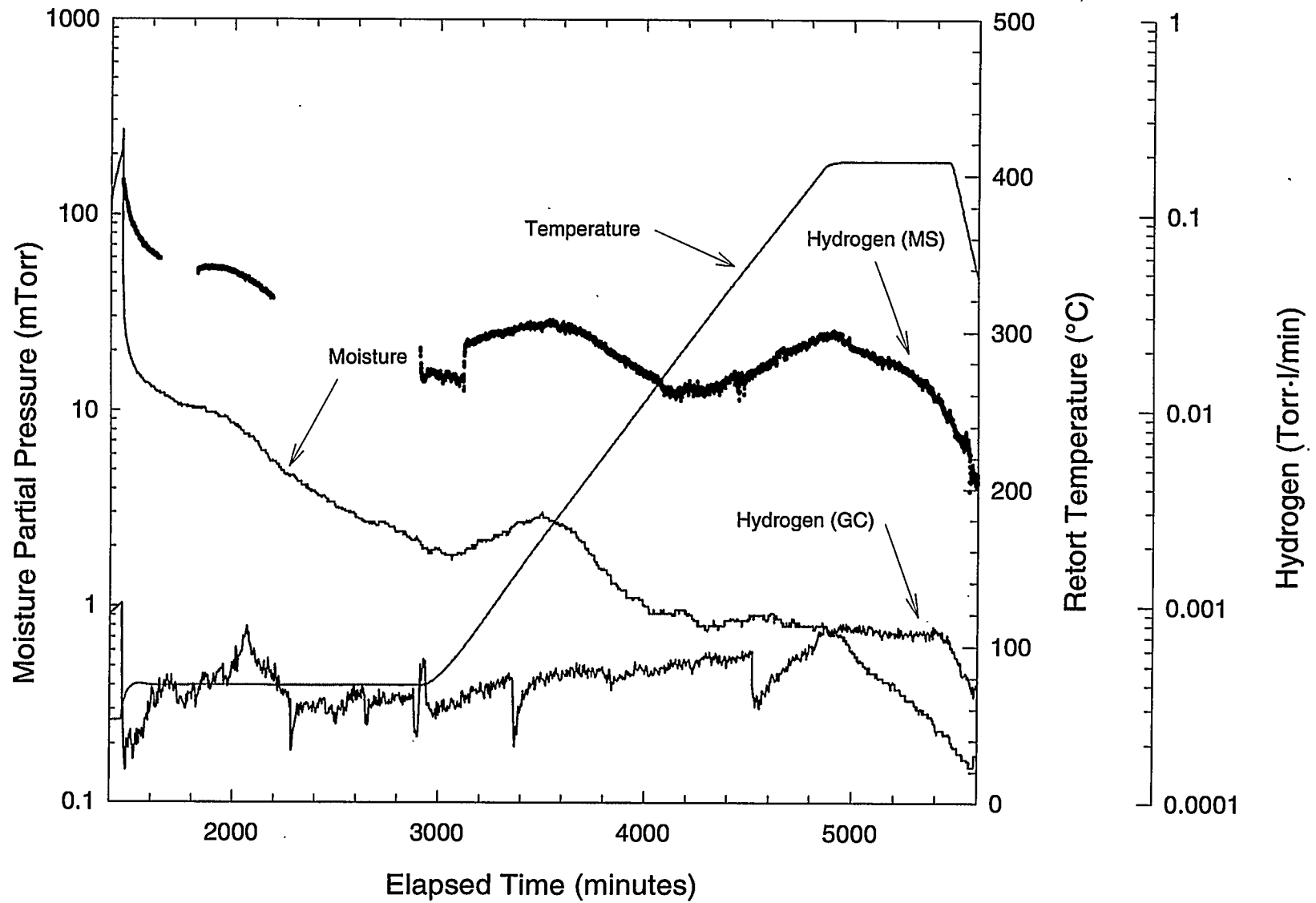


Figure 4.9. Spent Fuel Drying System Test Results, Hydrogen Release During HVD and Cooldown

Other than this slow increase, no trends were observed in the hydrogen signal. Approximately 1.5 Torr-l (~0.2 mg) of hydrogen was released during the entire HVD process over a time period of ~67 hours.

#### **4.5 Mass Spectrometer Measurements**

The drying system was designed so that the Balzers Omnistar MS could be used in conjunction with the GC to collect hydrogen and other gas release data over the test run. Hydrogen release values from the MS are also shown in Figure 4.9. Because of technical problems with the MS, MS data are missing for two segments of HVD. In contrast to the GC data, the MS hydrogen release values are higher and closely follow the moisture signal, with local maximum at ~170°C, and another at the maximum temperature of ~400°C. The close correlation of the hydrogen and water data suggest that the measured hydrogen in the MS is coming from local cracking of water by the MS source filament. Earlier tests, at much higher hydrogen levels, have shown good correlation between the GC and MS hydrogen data, with the GC values being somewhat higher.

## 5.0 Discussion

Ten milliliters of water were added to the element boat prior to the test. Of that, approximately 3 ml of water were observed in the condenser during the condenser pumpdown phase of CVD, somewhat higher than that calculated (~1.4 g) from Equation (3.1) over the same time period. The reason for the under-recovery of water in the condenser may be due to hang-up of water in colder sections of the system, particularly the particulate filters. Review of previous drying test data shows good correlation of fractional water recovery versus duration of the condenser pumpdown phase.

An additional ~1.0 mg of water was removed during the post-CVD Pressure Rise Test. This release can likely be interpreted as coming from free water that was trapped and not completely released during CVD. Approximately 10 ml of water were added to the system prior to the start of the test. Similar to earlier tests, the total pressure rise observed in the post-CVD test was only partially caused by residual moisture, suggesting that other sources of gas are responsible for some of the total pressure rise observed in the post-CVD test, even when no fuel element is present.

During the first segment of HVD, approximately 0.2 g of water was removed at temperatures between ~50°C and ~75°C. The second phase of HVD released approximately 0.05 g of water with a small peak at ~170°C. The final phase of HVD at 400°C released only about 4 mg of water, with an additional ~6 mg of water released during post-HVD cooldown. Consistent with previous tests, this indicates that small residual quantities of water remained even after the drying test was completed.

Most of the water removal after the post-CVD Pressure Rise Test occurred during the first phase of HVD, which entailed the temperature ramp from ~50°C to ~75°C. This water release is attributed to the release of water from isolated regions of the furnace system. This trend is similar to that observed during drying of fuel elements having additional isolated regions under the cladding.

Hydrogen data were obtained from the GC during the condenser pumpdown phase of CVD and during HVD. During the CVD period, approximately 0.001 mg of hydrogen was released, likely from outgassing of furnace components. During HVD, hydrogen showed only a slow increase, with no other trends. Approximately 0.2 mg of hydrogen was released during the entire HVD phase and, again, likely indicates background hydrogen outgassing levels for the furnace system.

In contrast to the GC data, MS hydrogen data during HVD showed higher levels that correlated closely with the moisture signal. Because of the close correlation with the moisture data, however, it is likely that the hydrogen signal is simply from cracking of water vapor by the MS source filament. Earlier tests at much higher hydrogen levels have shown good correlation between the GC and MS hydrogen data.

## 6.0 References

CRC Press. 1997. *Handbook of Chemistry and Physics*, 78<sup>th</sup> Edition. New York.

Ritter, G. A., S. C. Marschman, P. J. MacFarlan, and D. A. King. 1998. *Whole Element Furnace Testing System*. PNNL-11807, Pacific Northwest National Laboratory, Richland, Washington.

Westinghouse Hanford Company (WHC). 1995. *Hanford Spent Nuclear Fuel Project Integrated Process Strategy for K Basins Spent Nuclear Fuel*. WHC-SD-SNF-SP-005, Rev. 0, Richland, Washington.



## 7.0 Supporting Documents and Related Reports

Gerry, W. M. 1997a. *Calibration of Mass Flow Controllers*. SNF-TP-012, Rev. 0, Pacific Northwest National Laboratory, Richland, Washington.

Gerry, W. M. 1997b. *Calibration of Balzer Quadstar Mass Spectrometer*. SNF-TP-014, Rev. 0, Pacific Northwest National Laboratory, Richland, Washington.

Gerry, W. M. 1997c. *Calibration of MTI Gas Chromatograph Model M200*. SNF-TP-013, Rev. 0, Pacific Northwest National Laboratory, Richland, Washington.

Serles, J. A. 1997. *Wet/Dry Run Testing of G-Cell Furnace System in Preparation for Run #8 (6513U)*. 3M-TWD-PTL-013, Rev. 0, Pacific Northwest National Laboratory, Richland, Washington.

Reports are written separately for the whole element drying test series as follows:

Spent Fuel Drying System Test Results (First Dry-Run)

Spent Fuel Drying System Test Results (Second Dry-Run)

Spent Fuel Drying System Test Results (Dry-Run in Preparation for Run 8 [Third Dry-Run])

Drying Results of K-Basin Fuel Element 1990 (Run 1)

Drying Results of K-Basin Fuel Element 3128W (Run 2)

Drying Results of K-Basin Fuel Element 0309M (Run 3)

Drying Results of K-Basin Fuel Element 5744U (Run 4)

Drying Results of K-Basin Fuel Element 6603M (Run 5)

Drying Results of K-Basin Fuel Element 1164M (Run 6)

Drying Results of K-Basin Fuel Element 2660M (Run 7)

Drying Results of K-Basin Fuel Element 6513U (Run 8)

## Distribution

**No. of  
Copies**

**No. of  
Copies**

**OFFSITE**

C. L. Bendixsen  
Idaho National Engineering and  
Environmental Laboratory  
P.O. Box 1625  
Mail Stop 3135  
Idaho Falls, ID 83415

A. W. Conklin  
Washington State Department of Health  
Airdustrial Park  
Building 5, Mail Stop LE-13  
Olympia, WA 98504-0095

M. A. Ebner  
Idaho National Engineering and  
Environmental Laboratory  
P.O. Box 1625  
Mail Stop 3114  
Idaho Falls, ID 83415

A. R. Griffith  
U.S. Department of Energy, Headquarters  
19901 Germantown Rd (EM-65)  
Germantown, MD 20585-1290

T. J. Hull  
U.S. Department of Energy, Headquarters  
19901 Germantown Road (EH-34)  
Germantown, MD 20874-1290

M. R. Louthan  
Savannah River Technology Center  
Materials Technology Center  
Aiken, SC 29808

T. E. Madey  
Rutgers University  
Bldg. 3865  
136 Freylinghuysen Rd  
Piscataway, NJ 08854

B. K. Nelson  
U.S. Department of Energy, Headquarters  
19901 Germantown Road (EM-65)  
Germantown, MD 20874-1290

R. G. Pahl, Jr.  
Argonne National Laboratory  
P. O. Box 2528  
Idaho Falls, ID 83403

R. S. Rosen  
Lawrence Livermore National Laboratory  
20201 Century Blvd., 1<sup>ST</sup> Floor  
Germantown, MD 20874

D. Silver  
Washington State Department of Ecology  
P.O. Box 47600  
Olympia, WA 98504-7600

T. A. Thornton  
Yucca Mountain Project M&O Contractor  
SUM1/423  
1261 Town Center Drive  
Las Vegas, NV 89134

**No. of  
Copies**

**No. of  
Copies**

**ONSITE**

**2 Fluor Daniel Northwest**

**6 DOE Richland Operations Office**

R. M. Hiegel S7-41  
P. G. Loscoe S7-41  
C. R. Richins K8-50  
E. D. Sellers S7-41  
J-S. Shuen S7-41  
G. D. Trenchard S7-41

L. J. Garvin R3-26  
G. A. Ritter H0-40

**7 Numatec Hanford Company**

G. P. Chevrier H5-25  
T. Choho R3-86  
E. R. Cramer H0-34  
T. A. Flament H5-25  
J. J. Irwin R3-86  
C. R. Miska R3-86  
J. P. Slougher H5-49

**22 Duke Engineering and Services,  
Hanford, Inc.**

C. B. Aycock R3-11  
R. B. Baker H0-40  
D. W. Bergmann X3-79  
S. A. Chastain H0-40  
D. R. Duncan R3-86  
J. R. Frederickson R3-86  
L. H. Goldmann R3-86  
S. L. Hecht H0-40  
B. J. Makenas H0-40  
A. L. Pajunen R3-86  
R. W. Rasmussen X3-85  
A. M. Segrest R3-11  
J. A. Swenson R3-11  
C. A. Thompson R3-86  
D. J. Trimble (5) H0-40  
D. J. Watson X3-79  
J. H. Wicks, Jr. X3-74  
SNF Project Files R3-11

**2 Technical Advisory Group**

J. C. Devine R3-11  
R. F. Williams R3-11

**32 Pacific Northwest National Laboratory**

J. Abrefah (7) P7-27  
J. P. Cowin K8-88  
S. R. Gano K2-12  
W. J. Gray P7-27  
B. D. Hanson P7-27  
G. S. Klinger P7-22  
D. K. Kreid K7-80  
P. J. MacFarlan P7-27  
S. C. Marschman (5) P7-27  
B. M. Oliver P7-22  
R. P. Omberg K7-80  
T. M. Orlando K8-88  
L. R. Pederson K2-44  
J. K. Tarantino K9-41  
J. C. Wiborg K7-74  
Information Release (7)

**3 Fluor Daniel Hanford**

E. W. Gerber R3-11  
D. A. Smith T4-13  
M. J. Wiemers R3-11